Journal Pre-proofs

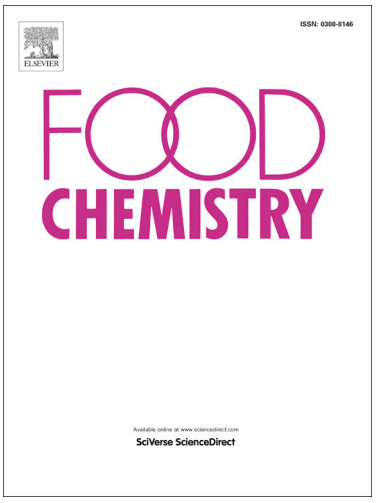

Proteomic and metabolomic basis for improved textural quality in crisp grass carp (*Ctenopharyngodon idellus* C.et V) fed with a natural dietary pro-oxidant

Ermeng Yu, Bing Fu, Guangjun Wang, Zhifei Li, Dewei Ye, Yong Jiang, Hong Ji, Xia Wang, Deguang Yu, Hashimul Ehsan, Wangbao Gong, Kai Zhang, Jingjing Tian, Lingyun Yu, Zhiyi Hu, Jun Xie, Gen Kaneko

PII: S0308-8146(20)30768-8
DOI: https://doi.org/10.1016/j.foodchem.2020.126906
Reference: FOCH 126906

To appear in: *Food Chemistry*

Received Date: 27 September 2019
Revised Date: 16 April 2020
Accepted Date: 23 April 2020

Please cite this article as: Yu, E., Fu, B., Wang, G., Li, Z., Ye, D., Jiang, Y., Ji, H., Wang, X., Yu, D., Ehsan, H., Gong, W., Zhang, K., Tian, J., Yu, L., Hu, Z., Xie, J., Kaneko, G., Proteomic and metabolomic basis for improved textural quality in crisp grass carp (*Ctenopharyngodon idellus* C.et V) fed with a natural dietary pro-oxidant, *Food Chemistry* (2020), doi: https://doi.org/10.1016/j.foodchem.2020.126906

Proteomic and metabolomic basis for improved textural quality in crisp grass carp (*Ctenopharyngodon idellus* C.et V) fed with a natural dietary pro-oxidant

Ermeng Yu[a,1], Bing Fu[a,1], Guangjun Wang[a], Zhifei Li[a], Dewei Ye[c], Yong Jiang[d], Hong Ji[e], Xia Wang[f], Deguang Yu[a], Hashimul Ehsan[b], Wangbao Gong[a], Kai Zhang[a], Jingjing Tian[a], Lingyun Yu[a], Zhiyi Hu[d], Jun Xie[a,*], Gen Kaneko[b,*]

[a] *Pearl River Fisheries Research Institute, Chinese Academy of Fishery Sciences, Guangzhou 510380, China*

[b] *School of Arts & Sciences, University of Houston-Victoria, Victoria, TX 77901, USA*

[c] *Joint Laboratory between Guangdong and Hong Kong on Metabolic Diseases, Guangdong Pharmaceutical University, Guangzhou 510006, China*

[d] *No.1 Affiliated Hospital of Guangzhou University of Chinese Medicine, 510405, China*

[e] *College of Animal Science and Technology, Northwest A&F University, Yangling 712100, China*

[f] *Department of Molecular and Cellular Biology, University of Arizona, Tucson, AZ 85721, USA*

* Correspondence: GK (email: KanekoG@uhv.edu), 3007 N Ben Wilson, Victoria, TX 77901, USA, or to EY (yem@prfri.ac.cn) or to JX (email: xiejunhy01@126.com), Pearl River Fisheries Research Institute, Chinese Academy of Fishery Sciences, Guangzhou 510380, China.

[1] These authors have contributed equally to this work.

ABSTRACT

Reactive oxygen species (ROS) regulate metabolism and chemical composition of various tissues. To understand how ROS affect the textural quality of fish muscle, we performed a multi-omics analysis on an established crisp grass carp model fed with a natural pro-oxidant faba bean. ROS levels were systemically and significantly increased up to three-fold in crisp grass carp, improving the muscle texture. Lipid metabolism was significantly enhanced up to five-fold in muscle and liver possibly to compensate the impaired carbohydrate metabolism of these tissues, but this caused further local ROS production. Mitochondrial damage associated with autophagy was evident in crisp grass carp. Proteomics revealed that elevated ROS likely disturbed the actin-myosin interaction and collagen turnover inducing fragmentation of myofibrillar proteins, all of which could have positively impacted the textural quality. The systemic metabolic changes that lead to the partial collapse of redox regulation likely underlie the ROS-induced improvement of textural quality.

Keywords:

Grass carp

Metabolism

Pro-oxidant

Redox

Textural quality

1. Introduction

The annual global growth in fish consumption has been twice as fast as population growth since 1961, demonstrating the critical importance of fish to achieve the FAO's goal of a world without hunger and malnutrition (FAO, 2018). Since fish products are highly vulnerable and perishable, ensuring fillet quality is significant for better consumer acceptance and active international trade (Cheng, Sun, Han & Zeng, 2014). Texture is one of the most important quality indicators of fish, and better texture also makes fish easy to process into high quality products (Hyldig & Nielsen, 2001). Factors affecting fish textural quality include chemical factors (fat content and distribution, carbohydrate content, muscle proteins, and collagen content), physical factors (feeding ingredients and species), and diverse treatments (freezing and high-pressure processing) (Pearce, Rosenvold, Andersen & Hopkins, 2011). The existing texture defects, such as muscle softening, are actually mostly attributed to changes of chemical compositions and the degradation of muscle proteins (Aussanasuwannakul, Kenney, Brannan, Slider, Salem & Yao, 2010). However, given the strong association of these factors with complex fish metabolism, the regulatory mechanism for fish textural quality is still not fully understood.

Reactive oxygen species (ROS) are an important regulator of muscle metabolism and therefore must influence the textural quality of fish muscle. Indeed, excess or insufficient levels of ROS are known to affect the textural quality of beef and broiler muscle possibly by interfering with collagen turnover in muscle fibroblasts (Chen, Zhang, Li, Gao & Zhou, 2017; Archile-Contreras & Purslow, 2011), whereas physiological levels of ROS are required for normal muscle development since they are involved in regulation of cell signaling pathways and the control of numerous redox-sensitive transcription factors (Powers, Ji, Kavazis, & Jackson, 2018). Some studies further pointed out that ROS regulate glucose and lipid metabolism, which play vital roles in the regulation of muscle quality and mass through modulating muscle cell growth, proliferation, and/or differentiation (Nemes, Koltai, Taylor, Suzuki, Gyori & Radak, 2018). ROS also affect the composition of metabolites, for example as the major initiator of lipid peroxidation that causes quality change in meat products (Min & Ahn, 2005). Although these studies have explored the role of ROS in the

regulation of muscle textural quality, the evidence remains fragmentary due to the different experimental models and methodologies. Therefore, a comprehensive proteomics and metabolomics study on a single established fish model would contribute to detect important textural and metabolic changes induced by ROS, especially those related to myofibrillar proteins and collagen, which will help to further explore the regulatory mechanism of ROS on fish textural quality.

Grass carp (*Ctenopharyngodon idellus*) is the largest aquaculture species, and its global production of 6.07 million tons accounts for 11% of worldwide finfish aquaculture production in 2016 (FAO, 2018). The introduction of crisp grass carp variety (*Ctenopharyngodon idellus* C.et V) as a high-value commodity product was one of the most important developments in the aquaculture industry. In crisp grass carp, the muscle firmness and springiness are increased significantly by feeding with faba bean (*Vicia faba* L.) solely for 90–120 days (Yu et al., 2014). Faba bean is rich in two glucosidic aminopyrimidine derivatives (vicine and convicine), which lead to the production of ROS such as hydrogen peroxide (H_2O_2) (Winterbourn, Benatti & De Flora, 1986), and therefore ROS possibly contribute to the textural quality change in crisp grass carp.

The overall objective of this study is to examine the redox regulation of carbohydrate and lipid metabolism in crisp grass carp with a particular attention to muscle textural quality. To this end, we employed a large-scale systemic approach on skeletal muscle, blood and liver because the metabolism of liver is an important factor to impact the development of skeletal muscle (i.e., liver-muscle crosstalk) (Pedersen & Febbraio, 2010). We specifically hypothesized that the dietary pro-oxidant faba bean induces systemic changes in proteomic and metabolomic profiles that are related to the improved textural quality in crisp grass carp.

2. Materials and methods

2.1. Animal culture, experimental diets and tissue collection

The feeding experiment was carried out in six tanks (4 m × 4 m × 1.5 m) located in the Pearl

River Fisheries Research Institute (Guangdong, China). One hundred and eighty individuals of grass carp, with an initial weight of 1782 ± 85 g (mean ± SD), were randomly divided into ordinary grass carp and crisp grass carp groups, with three replicates per treatment group. Ordinary grass carp were fed with formulated diet, and crisp grass carp were fed solely with faba beans. Faba bean contained dry matter 882 g/kg, crude protein 287 g/kg, and crude lipid 23.1 g/kg, whereas the formulated diet contained dry matter 911 g/kg, crude protein 360 g/kg, and crude lipid 36.2 g/kg. After 120 days, final weights for crisp grass carp and ordinary grass carp were 3926 ± 282 g and 4857 ± 219 g, respectively. Five individuals from each group were handled according to the procedures approved by the Malmo-Lund Ethical Committee, and individually euthanized in pH-buffered tricaine methanesulfonate (250 mg/L) (Dr. Ehrenstorfer, Augsburg, Germany). A variety of tissues were collected for the following analysis. Muscle and liver tissues were stored at -80 °C for gene expression analysis and for the measurement of physiological and biochemical parameters. Some of muscle and liver samples were fixed in 10% formalin for H&E staining. The metabolic and proteomic profiling were performed using three crisp grass carp and three ordinary grass carp. Blood was used for measurement of physiological and biochemical parameters.

Blood sample was taken from the tail vein of fish using a 5 mL sterile syringe, stored in a 10 mL sterile centrifuge tube at 4 °C for 3 h, and then centrifuged at 3500 × g for 10 min. The serum was used for the determination of blood parameters. On the other hand, approximately 8 ml of whole blood was collected for blood cell analysis. Whole blood was centrifuged at 2000 × g for 15 min, and plasma was separated and stored at −80°C. White blood cells were then collected and placed into fresh tubes, re-suspended in phosphate buffered saline (PBS), and centrifuged at 300×g for 10 min. Red blood cells were collected and stored at -80°C until further analyses.

2.2. Measurement of textural quality parameters

For texture analysis, fillets were taken from the junction of the fifth dorsal fin and the lateral line scales of grass carp back muscle. The muscle samples were examined using a Universal TA Texture Analyzer (Tengba instrument company, Shanghai, China) (Ma et al., 2020). The measured parameters include firmness (hardness) (g), chewiness (g), springiness, gumminess (g), and shear force (g). Collagen content was determined by the Kit No. A064-1 (Nanjing Jiancheng

Bioengineering Institute, Nanjing, China).

The evaluation of sensory tenderness was conducted by five experienced experts in sensory evaluation of crisp grass carp products who have at least 5 years of experience (male, ages 35–50) (Yang et al., 2015). The muscle sample was cut into 2 × 2 × 2 cm^3, placed in the water of 100 °C for 10 min, and then cooled down to room temperature for the sensory testing. Before evaluating each sample, every expert had to rinse their mouth with water for 5 times to reduce the interaction between the samples. An 8-point intensity scale was used (1~3 = flesh is less tender, 4~6 = flesh is moderate tender, 6~8 = flesh is tender).

2.3. H&E and oil red O staining of skeletal muscle and liver

The haematoxylin-eosin (H&E) staining was carried out on 3-mm-thick tissue blocks of muscle and liver according to the standard histology protocol. For the determination of muscle fiber diameter and density, the muscle fiber area within a certain field of view was measured, and the number of muscle fibers within the field were counted using the DP2-BSW 2.2 software (build 6212, Olympus, Tokyo, Japan). This method assumes that muscle fibers are cylindrical (Lee & Alexandra, 2001), and thus the diameter was calculated according to $s = \pi r^2$ (where s is the muscle fiber area and r is the muscle fiber radius). A total of 500 muscle fibers were analyzed for each sample. In addition, the oil red O staining of liver sample was performed according to Mehlem, Hagberg, Muhl & Eriksson (2013).

2.4. Proteomic profiling

Proteomic profiling of muscle and liver was performed as described previously (Yu et al., 2017). Briefly, the procedures included four main steps. (1) Preparation of the protein extract. Pooled samples were homogenised with a Dounce homogeniser (Wheaton Co., Wheaton, MO, USA) in a solution containing 6 M guanidine hydrochloride, 500 mM triethylammonium bicarbonate buffer and 0.1% Triton X-100 (Sigma Aldrich, St Louis, MO, USA). (2) iTRAQ labelling. Proteins (100 μg) were used for iTRAQ labelling following the manufacturer's protocols with an 8-plex iTRAQ kit (Applied Biosystems, Foster, CA, USA). (3) HPLC fractioning. Each labelled protein sample was fractionated on an SCX column using an Ultimate 3000 HPLC system (Dionex, Sunnyvale,

CA, USA). (4) Nano LC-MS/MS. The fraction was separated on a PicoFrit column (BioBasic C18, 75 μm × 10 cm, tip 15 μm; New Objective, Woburn, MA, USA) using an Ultimate 3000 nano-HPLC system (Dionex, Sunnyvale, CA, USA) in tandem with a nano-ESI-QqTOF (QStar Pulsar i, Applied Biosystems) with an ACN gradient. The data were acquired and analyzed using the Analyst QS version 1.1 software (Applied Biosystems). The protein numbers were identified using the UniProtKB database (http://www.uniprot.org). Comparing the experimental and control groups, proteins showing at least twofold differential expression (ratio < 0.5 or > 2) with $P < 0.05$ were selected and analyzed. Gene Ontology (GO) was identified by UniProtKB protein annotations (http://www.uniprot.org). The annotations of the signalling pathways were obtained by the KO database (http://www.genome.jp/kegg/ko.html). Protein–protein interaction network analysis was performed using the STRING database (V10) (http://string-db.org) and the Medusa software (https://sites.google.com/site/medusa3visualization).

2.5. Metabolic profiling

Liquid chromatography–mass spectrometry (LC-MS) analysis was performed using an UHPLC system (1290, Agilent Technologies, Santa Clara, CA, USA) with a UPLC HSS T3 column (1.8 μm, 2.1 mm × 100 mm, Waters) coupled to Q Exactive (Orbitrap MS, Thermo Fisher Scientific, Waltham, MA, USA). The mobile phase, consisted of positive (A: 0.1% formic acid in water; B: acetonitrile) and negative (A: 5 mM ammonium acetate in water; B: acetonitrile), was used for elution at 0.5 μL/min in the following gradient: 0 min, 1% B; 1 min, 1% B; 8 min, 99% B; 10 min, 99% B; 10.1 min, 1% B; 12 min, 1% B. The injection volume was 1 μL. The QE mass spectrometer was used for its ability to acquire MS/MS spectra on an information-dependent basis (IDA), and the acquisition software Xcalibur 4.0.27 (Thermo Fisher Scientific) continuously evaluated the MS data with ESI source in positive or negative modes. Gas chromatography–mass spectrometry (GC-MS) analysis was performed using an Agilent 7890 (Agilent Technologies) and a DB-5MS capillary column coated with 5% diphenyl cross-linked with 95% dimethylpolysiloxane (30 m × 250 μm inner diameter, 0.25 μm film thickness; J&W Scientific, Folsom, CA, USA). A 1 μL aliquot of the analyte was injected in splitless mode. Helium was used as the carrier gas with the front inlet purge flow of 3 mL/min, and the gas flow rate through the column of 1 mL/min. The initial temperature

was kept at 50 °C for 1 min, raised to 310 °C at a rate of 10 °C/min, and then kept for 8 min. The injection, transfer line, and ion source temperatures were 280, 280, and 250 °C, respectively. The energy was -70 eV in electron impact mode. The mass spectrometry data were acquired in full-scan mode with the m/z range of 50-500 at a rate of 20 spectra per second after a solvent delay of 6.27 min.

Raw data (LC-MS) were converted to the mzML format using ProteoWizard and processed by the R package XCMS (version 3.2). GC-MS raw data were analyzed using the Chroma TOF 4.3X software of LECO Corporation and LECO-Fiehn Rtx5 database (Smith, Want, O'Maille, Abagyan & Siuzdak, 2006). A variable importance in projection (VIP) scoring was applied to rank the metabolites that best distinguished between two groups. Those with *P* value of *t*-test < 0.05 and VIP ≥ 1 were considered differential metabolites between two groups. KEGG pathway of metabolites were analyzed by the major public pathway-related database (Okuda et al., 2008), and the calculated *P* values after the FDR correction were used to detect statistical significance with a threshold of 0.05. The chemical class, molecular formula and ID (HMDB) of differential metabolites were detected on HMDB Version 4.0 of Human Metabolome Database (http://www.hmdb.ca).

2.6. Measurement of H_2O_2, G6PD, NADPH/NADP$^+$, GSH/GSSG

The levels of H_2O_2 were examined by using a H_2O_2 assay kit (Abcam Plc., Cambridge, UK). Glucose-6-phosphate dehydrogenase (G6PD) activity was detected using a commercial kit by the colorimetric assay (Sigma-Aldrich).The ratio [reduced nicotinamide adenine dinucleotide phosphate (NADPH)]/[nicotinamide adenine dinucleotide phosphate (NADP$^+$)] was measured by a commercial NADPH/NADP+ quantification kit (Sigma-Aldrich). For blood sample, the NADPH/NADP+ ratio was measured by Kit No. A115-1 (Nanjing Jiancheng Bioengineering Institute). The detection of reduced glutathione in muscle or liver sample was performed using the [glutathione (GSH)]/[glutathione disulfide (GSSG)] Ratio Detection Assay Kit (Abcam). Serum was treated by a Deproteinization Sample Kit (Abcam) to remove proteins and analyzed by the same processes as muscle and liver samples.

2.7. Measurement of blood cells, lipid and glucose indexes

Blood white cells, red cells, platelet counts, and haemoglobin and mean corpuscular haemoglobin concentrations were measured using a haematology analyzer (Mek-7222K, Nihon Kohden, Tokyo, Japan). The Detection Kits from Nanjing Jiancheng Bioengineering Institute (Nanjing, China) were used to analyze contents of triglycerides (TG) (Kit No. A110-1), total cholesterol (TC) (Kit No. A111-1), high density lipoprotein cholesterol (HDLC) (Kit No. A112-1), low density lipoprotein cholesterol (LDLC) (Kit No. A113-1) from blood and liver samples. The levels of glucose were examined by using a glucose assay kit (F006-1-1, Nanjing Jiancheng Bioengineering Institute). The insulin and glucagon contents were determined using an insulin immunoassay kit (32100, AIS, Hong Kong, China) and a glucagon immunoassay kit (DGCG0, R&D Systems, Minneapolis, MN, USA), respectively.

2.8. Real-time PCR

According to the transcriptome data of grass carp (Yu, Bai, Fan, Ma, Quan & Jiang, 2015), primers were designed for the genes encoding Uncoordinated 51-Like Kinase 1 (Ulk1), Bcl-2 Nineteen-kilodalton Interacting Protein 3 (Bnip3), Parkin RBR E3 ubiquitin protein ligase (Park2), Cathepsin-L (Ctsl), Beclin1, carnitine palmitoyltransferase 1B (Cpt1b), short chain acyl-CoA dehydrogenases (Acads), long chain acyl-CoA dehydrogenases (Acadl), and β-actin (Table S4). Real-time PCR analysis was performed with a StepOnePlus™ Real-Time PCR System (Life Technologies, Waltham, MA, USA) using the Power SYBR Green Master Mix (Applied Biosystems). The cDNA was synthesized by using a cDNA Synthesis Kit (TaKaRa, Kusatsu, Japan). The reactions were performed in a 20 μL volume containing 1 μL of cDNA template, 10 μL of SYBR Mix, 0.2 μL of the forward and reverse primers (10 pmol/L) and 8.6 μL of ddH_2O. The reaction conditions were 50 °C for 2 min followed by 95 °C for 2 min and 40 cycles at 95 °C for 15 s, 58 °C for 30 s and 72 °C for 30 s. A denaturing step at 95 °C for 15 s was added after amplification, and a melting curve analysis was performed at the end of the assay over a range of 60–95 °C to verify that a single PCR product was generated. For normalization of cDNA loading, all samples were run in parallel with the reference gene (β-actin) in the same plate. The relative gene expression was calculated by the comparative CT method.

2.9. Western blot analysis

The protein extraction was performed with a protein extraction kit (Sangon Biotech, Shanghai, China). The proteins were separated on 6% SDS gels (30 μg per sample) and semidry-blotted onto PVDF membranes (Immobilon P; Millipore, Burlington, NJ, USA). After blocking with 5% BSA in TBST for 1 h, the membrane was incubated at room temperature for 30 min, and overnight at 4 °C with following antibodies in blocking buffer: rabbit anti-Complex I (Mt-Nd1) (1:1500), anti-Complex II (UQCRC1) (1:1500), anti-Bnip3 (1:1500), anti-[marker of sustained autophagy (LC3B)] (1:1500), anti-[central inducer of mitochondrial biogenesis (PGC1α)] (1:1000), anti-β-actin (1:1000), and mouse anti-Gapdh (1:1000), anti-Park2 (1:1500), anti-Complex IV (Mt-Co1) (1:1000), anti-Complex IV (Mt-Co2) (1:1500). The all antibodies were purchased from Abcam Company. The membrane was washed 5 times for 3 min with TBST, incubated for 1 h with goat anti-rabbit IgG (H+L) HRP (BBI Solutions, Crumlin, UK) (1:4000) in blocking buffer, and washed 6 times for 3 min with TBST. The membrane was then incubated for 5 min in ECL Plus (Amersham Biosciences, Piscataway, NJ, USA) and exposed to an X-ray film. The signal intensity was analyzed using the Quantity One software (Bio-Rad Laboratories Inc., Hercules, CA, USA). The relative expression was calculated as the ratio of gray values of the target and β-actin or Gapdh proteins (Yu et al., 2019).

2.10. Data analysis

All data were expressed as the mean ± SD. For all of the variables, after the normality of distribution was checked by the Shapiro-Wilk test, all data were demonstrated to be normally distributed. The homogeneity of variance was checked by the Levene's test. Statistical analyses were performed using the software SPSS 20.0 (SPSS Inc., Chicago, IL, USA). Data were analyzed by using the Student *t*-test. The *P* value less than 0.05 was considered to be statistically significant.

3. Results

3.1. Textural quality of skeletal muscle

In this study, we used the texture profile analysis (TPA), which simulates textural properties from chewing movement of human oral cavity (Wilkinson, Dijksterhuis & Minekus, 2000), to analyze the difference in texture property of crisp grass carp and ordinary grass carp. Compared with ordinary grass carp muscle, firmness, chewiness, springiness, gumminess, and shear force were higher in crisp grass carp muscle (Fig. 1A). Sensory tenderness was lower in crisp grass carp muscle (Fig. 1B) as expected from the known negative correlation between shear force and meat tenderness (Zhao et al., 2012).

Collagen content of crisp grass carp muscle was higher than that of ordinary grass carp (Fig. 1C). Microstructure observation further demonstrated that crisp grass carp has increased muscle fiber density (230 ± 15 No. /mm^2) compared with ordinary grass carp (183 ± 13 No. /mm^2) ($P < 0.05$) (Fig. 1D and E). In line with this, crisp grass carp exhibited lower muscle fiber diameters (88.26 ± 3.58 μm) than ordinary grass carp (101.26 ± 4.00 μm) ($P < 0.05$). These results extend our previous report about firmness and hyperplasia of crisp grass carp muscle (Yu et al., 2017).

3.2. Proteomics and metabolomics analysis of skeletal muscle and liver

In the proteomics analysis of skeletal muscle, we found a number of differentially expressed proteins: 21 proteins of muscle fiber structure (6 up- and 15 down-regulated), 1 down-regulated collagen precursor protein, 6 proteins of calcium ion binding (2 up- and 4 down-regulated), 42 redox-related proteins (13 up- and 29 down-regulated), 4 down-regulated proteins of carbohydrate metabolism, 16 proteins of lipid metabolism (3 up- and 13 down-regulated), and 37 other proteins [Fig. 2A; a preliminary analysis of this data has been published previously (Yu et al., 2017)]. The 42 differentially expressed redox-related proteins indicate that faba bean feeding affected the redox state, suggesting the importance of oxidation in the muscle quality improvement of crisp grass carp. Also, the differentially expressed proteins of muscle fiber structure, collagen and calcium likely contributed to the muscle textural quality improvement in crisp grass carp as summarized later in this paper taking other data into account. Overall, the above proteomics results demonstrate that

308 faba bean feeding affected the muscle redox state and metabolism, and these changes likely account
309 for the improved textural quality of skeletal muscle in crisp grass carp.

310 The subsequent LC-MS and GC-MS metabolomics detected 24 down-regulated and 39 up-
311 regulated metabolites in crisp grass carp muscle (vs. ordinary grass carp muscle) (Fig. 2C and Table
312 S1). Consistent with the proteomic changes observed above, many of down-regulated metabolites
313 were related to carbohydrate utilization (pyruvic acid, prunasin, thiophenecarboxaldehyde, etc.),
314 whereas increased metabolites included prenol lipid, indole and its derivatives, purine and its
315 derivatives and lignan glycoside. Calcium ion (Ca^{2+}) was also increased.

316 The liver proteomics analysis identified 41 redox-related proteins of differential expression, 12
317 proteins of carbohydrate metabolism, and 11 proteins of lipid metabolism (Fig. 2B and Table S2).
318 In the protein network analysis, the oxidative activity protein network was connected to structural
319 constituent of hepatocyte protein network, which was down-regulated possibly reflecting the
320 oxidative damage (Fig. S1). Up-regulation of 11 proteins in the structural constituent of ribosome
321 protein network is likely to be related to regeneration of the damaged tissue. Notably, crisp grass
322 carp liver contained a significantly higher amount of acaca (acetyl-CoA carboxylase alpha) protein,
323 a key and the rate-limiting enzyme in fatty acid synthesis that bridges lipid and carbohydrate
324 metabolism, indicating the enhanced fatty acid synthesis from carbon skeletons (Fig. S1, Table S2).
325 Fatty acid β-oxidation appeared to be enhanced as well because there were 9 up-regulated proteins
326 in the oxidative activity protein network. In line with these alterations, the hepatic glycogenolysis
327 pathway was significantly inhibited in crisp grass carp.

328 In the subsequent metabolic profiling by LC-MS and GC-MS, 76 up-regulated and 35 down-
329 regulated metabolites were identified in crisp grass carp liver (Fig. 2D; Table S3). Lipid metabolites
330 were dominant among them: out of 25 lipid metabolites, there were 9 up-regulated and 4 down-
331 regulated fatty acids and their derivatives, 4 up-regulated and 1 down-regulated
332 glycerophospholipids, 1 up-regulated and 3 down-regulated steroids, and 3 up-regulated prenol
333 lipids in crisp grass carp.

334 Together, these multi-omics analyses illustrated the overall metabolic features in crisp grass carp,
335 which is characterized by the redox changes, suppressed carbohydrate metabolism, and enhanced
336 lipid metabolism.

337

338 *3.3. Redox changes and mitochondrial autophagy in skeletal muscle*

339 We subsequently performed a detailed analysis on the redox state and metabolism in skeletal
340 muscle and liver of crisp grass carp to further understand the biochemical changes related to the
341 improved textural quality. The skeletal muscle of crisp grass carp showed clear evidence of redox
342 changes. The G6PD activity, $NADPH/NADP^+$ and GSH/GSSG ratios were lower than those of
343 ordinary grass carp; the H_2O_2 level was higher (Fig. 3A).

344 The expressions of genes encoding three enzymes of fatty acid β-oxidation, carnitine
345 palmitoyltransferase 1B (Cpt1b) and (very) long chain (Acadl) and short chain (Acads) acyl-CoA
346 dehydrogenases, were higher in the muscle of crisp grass carp than those in ordinary grass carp (Fig.
347 3B). These results are consistent with the multi-omics analysis that illustrated the enhanced
348 utilization of fatty acid in crisp grass carp muscle. On the other hand, compared with ordinary grass
349 carp, we found decreased protein expressions of subunits of the mitochondrial electron transport
350 chain, including Mt-Nd1 (Complex I), UQCRC1 (Complex II), Mt-Co1 and Mt-Co2 (Complex IV),
351 in crisp grass carp (Fig. 3C). These data suggest that mitochondrial function is possibly impaired in
352 the skeletal muscle of crisp grass carp.

353 Examinations on the autophagy genes further supported the impaired mitochondrial function in
354 the skeletal muscle of crisp grass carp. Compared to ordinary grass carp, crisp grass carp had higher
355 expressions of Uncoordinated 51-Like Kinase 1 (Ulk1), Bcl-2 Nineteen-kilodalton Interacting
356 Protein 3 (Bnip3), Parkin RBR E3 ubiquitin protein ligase (Park2), and Beclin1 (Fig. 3D). Park2 is
357 known to be specifically involved in mitochondrial clearance. Together with the decreased
358 expression of PGC1α (central inducer of mitochondrial biogenesis), these results indicate the
359 increased autophagy and decreased biogenesis of mitochondria in the muscle of crisp grass carp.
360 Microtubule-associated protein 1A/1B-light chain 3B (LC3B, a marker of sustained autophagy) was
361 highly expressed, suggesting that autophagy may be continuously enhanced in crisp grass carp
362 muscle (Fig. 3E).

363

364 *3.4. Redox regulation of muscle textural quality*

365 In skeletal muscle, we observed decreased carbohydrate metabolism and enhanced fatty acid β-

oxidation (Fig. 4). The enhanced β-oxidation and impaired mitochondrial function associated with mitophagy likely led to excess ROS generation in the skeletal muscle of crisp grass carp, creating a vicious loop between oxidative stress and metabolic changes. These changes were consistent with the increased level of H_2O_2, decreased G6PD activity, and decreased ratios of NADPH/$NADP^+$ and GSH/GSSG in crisp grass carp. It is noted that muscle and hepatic H_2O_2 levels were several orders higher than that of blood (see below), indicating the endogenous origin of H_2O_2.

From the proteomics analysis, we found three potential mechanisms by which ROS improved the textural quality of skeletal muscle of crisp grass carp. First, elevated ROS likely disturbed calcium binding and impaired actin-myosin interaction, leading to the decrease of muscle fiber diameter. Second, ROS-mediated fragmentation of myofibrillar proteins could also have contributed to the decrease of tenderness. Third, ROS-induced disruption in collagen turnover increased collagen contents and promoted the firmness increase. Together, these data provide a possible molecular basis to explain how redox changes improve the muscle quality in crisp grass carp.

3.5. Redox changes and mitochondrial autophagy in the liver

Liver is the central organ of metabolism, and we observed several hepatic responses to faba bean feeding consistent with above-mentioned changes in skeletal muscle. The most significant feature of crisp grass carp liver was the severe steatosis characterized by a typical vacuolated appearance of lipid-laden hepatocytes in H&E-stained sections (Fig. 5A). The hepatic steatosis was further confirmed by the increased intrahepatic lipid visualized by oil red O staining. Consistent with the histological observations, the liver of crisp grass carp had higher contents of hepatic total lipid (HL), TG, and TC compared to ordinary grass carp liver (Fig. 5B). Increased HDLC and LDLC levels in crisp grass carp liver further indicated that lipid transport from the liver is also activated.

These features are likely to be related to the faba bean-derived oxidative stress because the liver of crisp grass carp showed higher G6PD activity, NADPH/$NADP^+$ and GSH/GSSG ratios compared to ordinary grass carp. Crisp grass carp also had higher H_2O_2 level than ordinary grass carp in the liver (Fig. 5C).

The enhanced β-oxidation is likely to be peroxisomal because protein expressions of peroxisomal biogenesis factor (pex11b), peroxisomal membrane protein (pxmp2) and sterol carrier protein

395 (scp2a) were all significantly up-regulated in crisp grass carp liver (Fig. S2; Table S2); on the other
396 hand, protein expressions of subunits of the mitochondrial electron transport chain were decreased
397 except for Mt-Nd1 (Complex I) (Fig. 5D).

398 Examinations on the autophagy genes further supported the impaired mitochondrial function in
399 the liver of crisp grass carp. Compared to ordinary grass carp, crisp grass carp had higher hepatic
400 expressions of Ulk1, Bnip3, and Park2 (Fig. 5E). Other autophagy genes, Ctsl and Beclin1, also
401 showed an increasing tendency. The expression of PGC1α was significantly lower in crisp grass
402 carp liver. These results are quite similar to those in skeletal muscle, indicating the increased
403 autophagy and decreased biogenesis of mitochondria. LC3B, a marker of sustained autophagy, was
404 also highly expressed in crisp grass carp liver (Fig. 5F).

405 The overall liver metabolic features were deduced from biochemical indexes, microstructure, and
406 metabolic profiling results including proteomics and metabolomics, focusing on carbohydrate
407 metabolism, lipid metabolism and ROS production (Fig. S2). In crisp grass carp liver, carbohydrate
408 metabolism was severely suppressed with a concomitant up-regulation of fatty acid biosynthesis,
409 leading to hepatic steatosis. Mitochondrial damages were obvious. Peroxisomal β-oxidation was up-
410 regulated possibly to compensate the impaired carbohydrate metabolism and mitochondrial β-
411 oxidation, but this caused further ROS release. These results are consistent with metabolic shift from
412 carbohydrate to fatty acid utilization observed in muscle (e.g., suppressed carbohydrate metabolism,
413 enhanced β-oxidation in muscle).

414

415 *3.6. ROS, glucose, and hormone levels in the blood*

416 Lastly, we analyzed the blood of crisp grass carp to gain insights into the systemic redox changes
417 and the liver-muscle interaction. Compared to the blood of ordinary grass carp, crisp grass carp
418 blood had lower numbers of white cells, red cells, and platelets, as well as total haemoglobin and
419 mean corpuscular haemoglobin concentrations (Fig. S3A). Faba bean-induced oxidative stress is
420 likely to account for these changes because crisp grass carp (vs. ordinary grass carp) also
421 demonstrated low G6PD activity, low $NADPH/NADP^+$ ratio, low GSH/GSSG ratio and the high
422 H_2O_2 level (Fig. S3C). Importantly, crisp grass carp blood (vs. ordinary grass carp blood) had higher
423 contents of TG, TC and LDLC (liver-derived) (Fig. S3B). These results were in consistent with the

increased energy storage in the liver and enhanced β-oxidation in skeletal muscle of crisp grass carp. Blood glucose and glucagon levels were higher in crisp grass carp than ordinary grass carp, whereas there was no significant difference in the insulin levels (Fig. S2D).

3.7. Redox regulation and metabolic shift

In this study, our multi-system omics analysis illustrated the unique metabolic shift from carbohydrate to fatty acid utilization in skeletal muscle, liver, and blood (Fig. 6). Namely, carbohydrate metabolism was consistently down-regulated in these organs likely to be due to the faba bean-derived oxidative damage. Crisp grass carp appeared to have utilized fat as an alternative energy source as shown by enhanced β-oxidation in muscle, high blood TG/LDLC contents, and enhanced peroxisomal β-oxidation in the liver. However, the enhanced fat utilization further caused excess ROS accumulation of skeletal muscle along with elevated ROS levels in the blood and liver (Fig. 6). Together, our results demonstrated that ROS and ROS-induced metabolic changes play important roles in the increased textural quality of crisp grass carp.

4. Discussion

4.1. ROS-mediated regulation of muscle texture

Texture is one of the most important quality indicators of fish products, and understanding the biological processes involved in fish muscle texture will increase the production of value-added products and improve fishery profitability. In this study, textural quality of crisp grass carp muscle was better than that of ordinary grass carp with increased firmness, chewiness, springiness, gumminess, and shear force. Crisp grass carp muscle also showed increased collagen content and smaller muscle fiber diameter. Together with several previous findings (Yu et al. 2014; 2019), these results substantiate the concept that fish muscle firmness is positively correlated with collagen contents and negatively correlated with muscle fiber diameter. These changes in textural quality

452 must be attributed to the faba bean-derived oxidative stress, which altered the systemic redox
453 homeostasis as evidenced by changes in G6PD, GSH/GSSG, NADPH/$NADP^+$, and H_2O_2 levels.
454 Growing evidence indicates that structure and function of muscle fibers are impaired by
455 prolonged exposure to high levels of ROS (Yamada, Mishima, Sakamoto, Sugiyama, Matsunaga &
456 Wada, 2006). Myosin heavy chain proteins are targets of ROS, and oxidation of myosin heavy chain
457 proteins impairs their function (Zhou, Prather, Garrison & Zuo, 2018). Troponin C is also sensitive
458 to ROS-mediated oxidation (Ong & Steiner, 1997). In this study, proteomics of crisp grass carp
459 muscle identified 10 down-regulated proteins of muscle fiber structure, including myosin heavy
460 chain proteins, myosin light chain proteins, myosin binding proteins, actin protein, tropomyosin
461 protein, and troponin proteins. Down-regulation of myosin and actin suggests the impaired actin-
462 myosin interaction in crisp grass carp muscle, which decreases the muscle fiber diameter (Yu et al.,
463 2017). Also, it was recently reported that elevated ROS decrease myofibrillar Ca^{2+} sensitivity and
464 disturb calcium binding, which further impairs the actin-myosin interaction (Theofilidis, Bogdanis,
465 Koutedakis & Karatzaferi, 2018). This would be the case in crisp grass carp since we observed
466 disruption in the Ca^{2+} signaling in crisp grass carp muscle (4 down-regulated proteins of calcium
467 ion binding and concomitant increase in Ca^{2+}). In addition, ROS-induced disruption in collagen
468 turnover possibly increased collagen contents and firmness in crisp grass carp muscle in a similar
469 mechanism that ROS affected beef quality (Archile-Contreras & Purslow, 2011). Taken together,
470 we speculate that elevated ROS levels led to decreased muscle fiber diameter and disrupted collagen
471 turnover, contributing to the firmness increase of skeletal muscle in crisp grass carp.
472

473 *4.2. The systemic metabolic shift*

474 The most striking metabolic alteration in crisp grass carp was the systemic suppression of
475 carbohydrate metabolism associated with enhanced fatty acid β-oxidation. These results are in line
476 with the changes in blood hormone levels. Namely, crisp grass carp cannot efficiently utilize
477 nutrients glucose as demonstrated by the multi-omics analysis. The hormone balance was thus
478 catabolic as indicated by higher levels of glucagon, a hormone that increases blood glucose and
479 stimulates lipolysis associated with the β-oxidation (Galsgaard, Pedersen, Knop, Holst, &
480 Albrechtsen, 2019). Lipids released into the blood circulation system can probably be better utilized

481 than glucose, and thus the difference in blood glucose levels between crisp grass carp and ordinary
482 grass carp was more pronounced compared to that in blood lipid levels.
483 This metabolic shift may account for the low lipid content of crisp grass carp (Tian et al., 2019),
484 which is associated with muscle firmness in fish (Nielsen, Hyldig, Nielsen & Nielsen, 2005). The
485 increased VLDL in liver and blood indicates active lipid transport to skeletal muscle, but these lipids
486 are likely to be oxidized in the skeletal muscle by enhanced β-oxidation rather than being stored in
487 intramuscular adipose tissues. Importantly, liver is also the source of follistatin, a naturally occurring
488 inhibitor of myostatin (Hansen et al., 2011), whereas skeletal muscle secretes myokines that affect
489 the muscle–liver crosstalk, such as muscle-derived interleukin-6 (IL-6) that enhances hepatic
490 glucose uptake (Pedersen & Febbraio, 2010). Further investigation of such hormones and cytokines
491 will shed light on the muscle–liver crosstalk of crisp grass carp.
492
493 *4.3. Hepatic steatosis in crisp grass carp*
494 Another dramatic phenotypic alteration found in crisp grass carp is the hepatic steatosis.
495 Enhanced fatty acid β-oxidation appears to be contradictory to the hepatic steatosis, but this is likely
496 to be a compensation for impaired mitochondrial function by peroxisomes. In mammals,
497 mitochondrial β-oxidation is known to be dominant among the pathways for fatty acid oxidation,
498 whereas peroxisomal β-oxidation is involved in the metabolism of very long chain fatty acids and
499 branched-chain fatty acids that cannot directly undergo mitochondrial β-oxidation (Reddy &
500 Mannaerts, 1994). However, it is known in *Myoxocephalus octodecimspinosus*, a marine teleost
501 having relatively high carbohydrate utilization, that peroxisomal β-oxidation accounts for 50% of
502 fatty acid oxidation (palmitoyl-CoA substrate) (Crockett & Sidell, 1993). This ratio is high
503 compared to mammals, in which peroxisomal β-oxidation is responsible for only 32% to < 10% of
504 total fatty acid oxidation unless treated with peroxisomal proliferators. Fish peroxisomes may be
505 able to compensate the mitochondrial β-oxidation to a larger extent than do mammalian peroxisomes.
506 In the case of crisp grass carp, the compensatory peroxisomal β-oxidation would have contributed
507 to the improved textural quality by inducing systemic oxidative stress because peroxisomal β-
508 oxidation produces H_2O_2 as the final product.
509

510 *4.4. Potential effects of dietary pro-oxidants on human metabolism*

511 A potential implication of this study in human nutrition and metabolism is that the ROS-induced
512 changes in muscle quality. Increase in muscle mass by exercise is at least partly attributed to the
513 damages to muscle fibers, which was achieved by faba bean feeding in this study. Previous studies
514 have shown that faba bean exerts similar effects on muscle quality of mammals (Calabrò et al.,
515 2014; Milczarek et al., 2016). It is tempting to speculate that consuming dietary pro-oxidants upon
516 exercise may help in achieving better body shape in sports nutrition, although the pro-oxidant
517 content should be strictly controlled to avoid the detrimental metabolic effects. In case of crisp grass
518 carp, the content of vicine, an oxidative compound possibly responsible for the ROS-induced
519 changes, is around 1.5% (Ma et al., 2020), and the blood H_2O_2 concentration is ~0.6 pmol/μL. These
520 values will be the basis to develop future experimental plans for examining the beneficial and
521 detrimental effects of dietary pro-oxidant.

522 Another important implication of this study is favism. Faba bean is a widely consumed natural
523 pro-oxidant that causes a serious disease, favism, characterized by acute hemolysis (Luzzatto &
524 Arese, 2018). In general favism is observed only in people with glucose-6-phosphate dehydrogenase
525 (G6PD) deficiency because this enzyme is responsible for maintaining adequate levels of NADPH,
526 which protects the cell from oxidative stress. The G6PD deficiency is the most common human
527 enzyme defect found in more than 400 million people, which makes favism one of the ongoing
528 major health problems (Luzzatto & Arese, 2018). On the other hand, it is reasonable to assume that
529 faba bean intake has some detrimental (or beneficial) metabolic impacts on people without G6PD
530 deficiency because ROS is a well-known risk factor for developing metabolic disorders (Rani, Deep,
531 Singh, Palle & Yadav, 2016). However, such effects have rarely been investigated, possibly being
532 overlooked because of the severe symptom of favism. Only some reports have detected impaired
533 blood and liver functions in favism patients (Dorgalaleh et al., 2013). In this study, we identified
534 evidence of oxidative damages in various organs of crisp grass carp, and especially changes in blood
535 parameters reflect the symptoms of human favism. Other metabolic alterations in crisp grass carp,
536 such as suppression of carbohydrate metabolism and hepatic steatosis, may represent the
537 consequence of faba bean intake in people without G6PD deficiency. It is worth to investigate the
538 association between faba bean intake and metabolic parameters especially in Mediterranean and

Middle Eastern area where faba bean is a popular traditional food. It should be also noted that continuous efforts have been made to produce faba bean variations containing less oxidative compounds (O'Sullivan & Angra, 2016). Understanding the metabolic impact of traditional faba bean would accelerate the development, contributing to assurance of food safety.

5. Conclusions

In conclusion, this study demonstrated that faba bean improved the textural quality of crisp grass carp muscle. The multi-system omics analysis on crisp grass carp revealed the systemic oxidative damage and metabolic shift from carbohydrate to fatty acid utilization. The enhanced β-oxidation and mitophagy possibly result in further ROS generation in crisp grass carp. Elevated ROS led to decrease of muscle fiber diameter and tenderness and increase of firmness probably by disturbing calcium binding, impairing actin-myosin interaction, mediating fragmentation of myofibrillar proteins, and decreasing collagen turnover. Overall, ROS and ROS-induced metabolic changes play important roles in the improved the textural quality of crisp grass carp.

Author contributions

E.M. Yu, J. Xie and G. Kaneko conceived and designed the experiments. B. Fu, G. Wang, Z. Li, D. Yu, Y. Jiang, D.G. Yu, W.B. Gong, K. Zhang and J.J. Tian performed experimental biological research. H. Ji, X. Wang, H. Ehsan and Z.Y. Hu analyzed the data. L.Y. Yu provided the transcriptome data of grass carp. E.M. Yu, B. Fu and G. Kaneko co-wrote the paper. All authors reviewed or edited the manuscript.

Competing interests

The authors declare no competing interests.

Acknowledgments

We thank Qianyu Guo and Zhennan Zhang for technical support with H&E and oil red O staining and electron microscope. This study was funded by the Modern Agro-industry Technology Research System (No.CARS-45-21) and the National Natural Science Foundation of China (No. 31402312).

Appendix A. Supplementary data

Supplementary Information accompanies this paper were provided.

References

Archile-Contreras, A. C., & Purslow P. P. (2011). Oxidative stress may affect meat quality by interfering with collagen turnover by muscle fibroblasts. *Food Research International*, *44*(2), 582–588.

Aussanasuwannakul, A., Kenney, P. B., Brannan, R. G., Slider, S. D., Salem, M., & Yao J. (2010). Relating instrumental texture, determined by variable-blade and Allo-Kramer shear attachments, to sensory analysis of rainbow trout (*Oncorhynchus mykiss*) fillets. *Journal of Food Science*, *75*(7), S365–S374.

Calabrò, S., Cutrignelli, M. I., Gonzalez, O. J., Chiofalo, B., Grossi, M., Tudisco, R., Panetta, C., & Infascelli, F. (2014). Meat quality of buffalo young bulls fed faba bean as protein source. *Meat Science*, *96*, 591-596.

Chen X., Zhang, L., Li, J., Gao, F., & Zhou, G. (2017). Hydrogen peroxide-induced change in meat quality of the breast muscle of broilers is mediated by ROS generation, apoptosis, and autophagy in the NF-κB signal pathway. *Journal of Agricultural and Food Chemistry*, *65*(19), 3986–3994.

Cheng, J. H., Sun, D. W., Han, Z., & Zeng X. A. (2014). Texture and structure measurements and analyses for evaluation of fish and fillet freshness quality: A review. *Comprehensive Reviews in Food Science and Food Safety*, *13*(1), 52–61.

Crockett, E. L., & Sidell, B. D. (1993). Peroxisomal beta-oxidation is a significant pathway for catabolism of fatty acids in a marine teleost. *American Journal of Physiology - Regulatory, Integrative and Comparative Physiology*, *264*, R1004–R1009.

Dorgalaleh, A., Shahzad, M. S., Younesi, M. R., Moghaddam, E. S., Mahmoodi, M., Varmaghani, B., Khatib, Z. K, & Alizadeh, S. (2013) Evaluation of liver and kidney function in favism patients. *Medical Journal of the Islamic Republic of Iran, 27*, 17–22.

FAO. The State of World Fisheries and Aquaculture (2018). Meeting the sustainable development goals, Rome. Licence: CC BY-NC-SA 3.0 IGO.

Galsgaard, K. D., Pedersen, J., Knop, F. K., Holst, J. J., & Albrechtsen, N. J. W. (2019). Glucagon receptor signaling and lipid metabolism. *Frontiers in Physiology*, *10*, e413.

Hansen, J., Brandt, C., Nielsen, A. R., Hojman, P., Whitham, M., Febbraio, M. A., Pedersen, B. K., & Plomgaard, P. (2011). Exercise induces a marked increase in plasma follistatin: Evidence that follistatin is a contraction-induced hepatokine. *Endocrinology, 152*(1), 164–171.

Hyldig, G., & Nielsen, D. (2001). A review of sensory and instrumental methods used to evaluate the texture of fish muscle. *Journal of Texture Studies*, *32*(3), 219–242.

Lee, S. J. & Alexandra, C. M. (2001). Regulation of myostatin activity and muscle growth. *Proceedings of the National Academy of Sciences of the United States of America, 98*(16), 9306–9311.

Luzzatto, L. & Arese, P. Favism and glucose-6-phosphate dehydrogenase deficiency. (2018) *N Engl J Med*, *378*, 60–71.

Ma, L. L., Kaneko, G., Wang, X. J., Xie, J., Tian, J. J., Zhang, K., Wang, G. J., Yu, D. G., Li, Z. F., Gong, W. B., Yu, E. M., & Li, H. H. (2020). Effects of four faba bean extracts on growth parameters, textural quality, oxidative responses, and gut characteristics in grass carp. *Aquaculture*, *516*, 734620.

Mehlem, A., Hagberg, C. E., Muhl, L., Eriksson, U., & Falkevall A. (2013). Imaging of neutral lipids by oil red O for analyzing the metabolic status in health and disease. *Nature Protocols*, *8*(6), 1149–1154.

Milczarek, A., & Osek, M. (2016). Partial replacement of soybean with low-tannin faba bean varieties (Albus or Amulet): effects on growth traits, slaughtering parameters and meat quality of puławska pigs. *Nephron Clinical Practice*, *16*, 477-487.

Min, B., & Ahn, D. U. (2005). Mechanism of lipid peroxidation in meat and meat products - A review. *Food Science and Biotechnology*, *14*(1), 152–163.

Nemes, R., Koltai, E., Taylor, A., Suzuki, K., Gyori, F., & Radak, Z. (2018). Reactive oxygen and nitrogen species regulate key metabolic, anabolic, and catabolic pathways in skeletal muscle. *Antioxidants*, *7*(7), e85.

Nielsen, D., Hyldig, G., Nielsen, J., & Nielsen, H. H. (2005). Liquid holding capacity and instrumental and sensory texture properties of herring (*Clupea harengus* L.) related to biological and chemical parameters. *Journal of Texture Studies*, *36*(2), 119–138.

Okuda, S., Yamada, T., Hamajima, M., Itoh, M., Katayama, T., Bork, P., Goto, S., & Kanehisa, M. (2008). KEGG Atlas mapping for global analysis of metabolic pathways. *Nucleic Acids Research*, *36*, W423–W426.

Ong, S. H., & Steiner A. L. (1997). Localization of cyclic GMP and cyclic AMP in cardiac and skeletal muscle: immunocytochemical demonstration. *Science, 195*(4274), 183–185.

O'Sullivan, D. M. & Angra, D. (2016) Advances in faba bean genetics and genomics. *Frontiers in Genetics*, *7*, 150.

Pearce, K. L., Rosenvold, K., Andersen, H. J., & Hopkins, D. J. (2011). Water distribution and mobility in meat during the conversion of muscle to meat and ageing and the impacts on fresh meat quality attributes - A review. *Meat Science*, *89*(2), 111–24.

Pedersen, B. K., & Febbraio, M. A. (2012). Muscles, exercise and obesity: skeletal muscle as a secretory organ. *Nature Reviews in Endocrinology*, *8*(8), 457–465.

Powers, S. K., Ji, L. L., Kavazis, A. N., & Jackson M. J. (2011). Reactive oxygen species: impact on skeletal muscle. *Comprehensive Physiology*, *1*(2), 941–969.

Rani, V., Deep, G., Singh, R. K., Palle, K., & Yadav, U. C. S. (2016) Oxidative stress and metabolic disorders: pathogenesis and therapeutic strategies. *Life Sciences, 148*, 183–193.

Reddy, J. K., & Mannaerts, G. P. (1994). Peroxisomal lipid metabolism. *Annual Review of Nutrition*, *14*, 343–370.

Smith, C. A., Want, E. J., O'Maille, G., Abagyan, R., & Siuzdak, G. (2006). XCMS: processing mass spectrometry data for metabolite profiling using nonlinear peak alignment, matching, and identification. *Analytical Chemistry*, *78*(3), 779–787.

Theofilidis, G., Bogdanis, G., Koutedakis, Y., & Karatzaferi, C. (2018). Monitoring exercise-induced muscle fatigue and adaptations: Making sense of popular or emerging indices and biomarkers. *Sports*, *6*(4), e153.

Tian, J. J., Ji, H., Wang, Y. F., Xie, J., Wang, G. J., Li, Z. F., Yu, E. M., Yu, D. G., Zhang, K., & Gong W. B. (2019). Lipid accumulation in grass carp (*Ctenopharyngodon idellus*) fed faba beans (*Vicia faba* L.). *Fish Physiology and Biochemistry*, *45*(2), 631–642.

Wilkinson, C., Dijksterhuis, G. B. & Minekus, M. (2000). From food structure to texture. *Trends in Food Science and Technology*, *11*(12), 442–450.

Winterbourn, C. C., Benatti, U., & De Flora, A. (1986). Contributions of superoxide, hydrogen peroxide, and transition metal ions to auto-oxidation of the favism-inducing pyrimidine aglycone, divicine, and its reactions with haemoglobin. *Biochemistry & Pharmacology*, *35*(12), 2009–2015.

Yamada, T., Mishima, T., Sakamoto, M., Sugiyama, M., Matsunaga, S., & Wada, M. (2006). Oxidation of myosin heavy chain and reduction in force production in hyperthyroid rat soleus. *Journal of Applied Physiology*, *100*(5), 1520–1526.

677 Yang, S., Li, L., Qi, B., Wu, Y., Hu, X., Lin, W., Hao, S., & Huang, H. (2015). Quality evaluation
678 of crisp grass carp (*Ctenopharyngodon idellus* C. ETV) based on instrumental texture analysis
679 and cluster analysis. *Food Analytical Methods*, *8*(8), 2107–2114.
680 Yu, E., Xie, J., Wang, G., Yu, D., Gong, W., Li, Z., Wang, H., Xia, Y., & Wei, N. (2014). Gene
681 expression profiling of grass carp (*Ctenopharyngodon idellus*) and crisp grass carp.
682 *International Journal of Genomics*, *2014*, e639687.
683 Yu, E. M., Zhang, H. F., Li, Z. F., Wang, G. J., Wu, H. K., Xie, J., Yu, D. G., Xia, Y., Zhang, K.,
684 & Gong, W. B. (2017). Proteomic signature of muscle fibre hyperplasia in response to faba
685 bean intake in grass carp. *Scientific Reports*, *7*, e45950.
686 Yu, E. M., Ma, L. L., Ji, H., Li, Z. F., Wang, G. J., Xie, J., Yu, D. G., Kaneko, G., Tian, J. J., &
687 Zhang, K. (2019). Smad4-dependent regulation of type I collagen expression in the muscle of
688 grass carp fed with faba bean. *Gene, 685*, 32–41.
689 Yu, L., Bai, J., Fan, J., Ma, D., Quan, Y., & Jiang, P. (2015). Transcriptome analysis of the grass
690 carp (*Ctenopharyngodon idella*) using 454 pyrosequencing methodology for gene and marker
691 discovery. *Genetics and Molecular Research*, *14*(4), 19249–19263.
692 Zhao, C., Tian, F., Yu, Y., Luo, J., Hu, Q., Bequette, B. J., Baldwin Vi. R. L., Liu, G., Zan, L.,
693 Updike, M. S., & Song, J. (2012). Muscle transcriptomic analyses in Angus cattle with
694 divergent tenderness. *Molecular Biology Reports*, *39*(4), 4185–4193.
695 Zhou, T., Prather, E., Garrison, D., & Zuo, L. (2018). Interplay between ROS and antioxidants
696 during ischemia-reperfusion injuries in cardiac and skeletal muscle. *International Journal of*
697 *Molecular Sciences*, *19*(2), e417.

698

699

700

701 **Figure legends**

702

703 **Fig. 1.** Textural quality improvement of skeletal muscle in crisp grass carp. GC, ordinary grass carp;
704 CGC, crisp grass carp. (A) Muscle textural parameters. (B) Collagen content. (C) Microstructure

705 observation (×400). mf, muscle fiber. (D) Muscle fiber density and diameter. Statistical analyses
706 were performed using Student's *t*-test, * $P < 0.05$ and ** $P < 0.01$.
707
708 **Fig. 2.** Proteomics and metabolomics analysis of skeletal muscle and liver. GC, ordinary grass carp;
709 CGC, crisp grass carp. (A) Proteomics analysis of skeletal muscle. (B) Proteomics analysis of liver.
710 (C) Metabolomics analysis of skeletal muscle. Red for up-regulated and green for down-regulated.
711 (D) Metabolomics analysis of liver.
712
713 **Fig. 3.** Redox and metabolic changes associated with mitochondrial dysfunction and autophagy in
714 skeletal muscle of crisp grass carp. GC, ordinary grass carp; CGC, crisp grass carp. (A) Activity of
715 glucose-6-phosphate dehydrogenase (G6PD), ratios of NADPH/$NADP^+$, GSH/GSSG, and level of
716 hydrogen peroxide (H_2O_2). NADPH, reduced nicotinamide adenine dinucleotide phosphate; $NADP^+$,
717 nicotinamide adenine dinucleotide phosphate; GSH, glutathione; GSSG, glutathione disulfide. (B)
718 mRNA expression of enzymes involved in fatty acid β-oxidation. Cpt1b, carnitine
719 palmitoyltransferase 1B; Acads, short chain acyl-CoA dehydrogenases; Acadl, long chain acyl-CoA
720 dehydrogenases. (C) Protein expressions of mitochondrial complexes. (D) mRNA expressions of
721 autophagy genes including Uncoordinated 51-Like Kinase (Ulk1), Bcl-2 Nineteen-kilodalton
722 Interacting Protein 3 (Bnip3), Parkin RBR E3 ubiquitin protein ligase (Park2), and Beclin1. (E)
723 Expressions of autophagy proteins including Park2, Bnip3, peroxisome proliferator-activated
724 receptor gamma coactivator 1-alpha (PGC1α) and microtubule-associated protein 1A/1B-light chain
725 3B (LC3B). Statistical analyses were performed using Student's *t*-test, * $P < 0.05$ and ** $P < 0.01$.
726
727 **Fig. 4.** Redox regulation of metabolism and muscle textural quality in crisp grass carp. GC, ordinary
728 grass carp; CGC, crisp grass carp. Abbreviations are as followings: **pdha1a**, pyruvate
729 dehydrogenase (lipoamide); **pc**, pyruvate carboxylase; **g6pd**, Glucose-6-phosphate 1-
730 dehydrogenase; **gsrm**, glutathione reductase, mitochondrial-like; **prdx6**, peroxiredoxin 6; **crt**,
731 calreticulin; **myl4**, myosin, light chain 4; **myl10**, myosin, light chain 10, regulatory; **tnnc1b**,
732 troponin C type 1b (slow); **mhc**, myosin heavy chain, fast skeletal muscle, partial; **smyhc1**, slow
733 myosin heavy chain 1; **mybpc1**, myosin-binding protein C, slow-type; **tnnt**, novel slow skeletal

734 troponin T family protein; **actin1**, muscle actin type 1; **neb**, novel protein similar to vertebrate
735 nebulin; **tpm2**, tropomyosin beta chain; **krt18**, keratin 18; **smyhc1**, slow myosin heavy chain 1;
736 **mybpc1**, myosin-binding protein C, slow-type; **col1a1p**, collagen, type I, alpha 1b precursor.
737
738 **Fig. 5.** Redox and metabolic changes associated with mitochondrial dysfunction and autophagy in
739 the liver of crisp grass carp. GC, ordinary grass carp; CGC, crisp grass carp. (A) H&E-stained
740 paraffin and oil red O-stained frozen sections. (B) Contents of triglyceride (TG), total cholesterol
741 (TC), high density lipoprotein cholesterol (HDLC), and low density lipoprotein cholesterol (LDLC).
742 (C) Activity of glucose-6-phosphate dehydrogenase (G6PD), the ratios of NADPH/$NADP^+$ and
743 GSH/GSSG, and level of hydrogen peroxide (H_2O_2). NADPH, reduced nicotinamide adenine
744 dinucleotide phosphate; $NADP^+$, nicotinamide adenine dinucleotide phosphate; GSH, glutathione;
745 GSSG, glutathione disulfide. (D) Protein expressions of mitochondrial complexes. (E) mRNA
746 expressions of autophagy genes including Ulk1, Bnip3, Park2, Cathepsin-L (Ctsl) and Beclin1. (F)
747 Expressions of autophagy proteins including Park2, Bnip3, PGC1α (Peroxisome proliferator-
748 activated receptor gamma coactivator 1-alpha) and LC3B (Microtubule-associated protein 1A/1B-
749 light chain 3B). Statistical analyses were performed using Student's *t*-test, * $P < 0.05$ and ** $P <$
750 0.01.
751
752 **Fig. 6.** Redox regulation and metabolic shift in crisp grass carp. Blue and red italic letters indicate
753 down- and up-regulations respectively. Black italic letters indicate observed physiological changes.
754 G6PD, glucose-6-phosphate dehydrogenase; NADPH, reduced nicotinamide adenine dinucleotide
755 phosphate; GSH, glutathione; H_2O_2, hydrogen peroxide; TG, triglycerides; TC, total cholesterol;
756 LDLC, low density lipoprotein cholesterol.
757
758 E.M. Yu, J. Xie and G. Kaneko conceived and designed the experiments. B. Fu, G. Wang, Z. Li,
759 D. Yu, Y. Jiang, D.G. Yu, W.B. Gong, K. Zhang and J.J. Tian performed experimental biological
760 research. H. Ji, X. Wang, H. Ehsan and Z.Y. Hu analyzed the data. L.Y. Yu provided the
761 transcriptome data of grass carp. E.M. Yu, B. Fu and G. Kaneko co-wrote the paper. All authors

762 reviewed or edited the manuscript.

763
764

765 **Highlights**

766 - Dietary pro-oxidant improved the textural quality of grass carp muscle
767 - ROS likely disturbed actin-myosin interaction and collagen turnover in the muscle
768 - ROS suppressed carbohydrate metabolism and enhanced fatty acid oxidation

769